First Results with RK-Time Integration and High-Order Spatial Discretization

Jochen Förstner, Günther Doms
Deutscher Wetterdienst, Frankfurter Straße 135, 63067 Offenbach am Main

1. Overview

Based on the work of Gaßmann (2002) new variants of 2-timelevel schemes were implemented into the LM. The time-integration is of Runge-Kutta type and is combined with high-order spatial discretization of the advection terms in the dynamical core. The implementation is done in a way one can easily switch between the Runge-Kutta schemes of 2nd- and 3rd-order (it is also possible to choose a simple Euler-forward scheme) as well as advection schemes of 3rd-order upwind, 4th-order centered and 5th-order upwind using namelist-parameters. This type of integration was suggested by Wicker and Skamarock (2002) and is currently implemented in the WRF. In contradiction to them the advection form and not the flux form is used - details of the discretization are given in the box below. Also implemented is a 3rd-order TVD variant of the Runge-Kutta scheme (Shu and Osher 1988).

Especially the results for the RK-3rd / UP-5th scheme are very promising. Whereas computational more demanding this scheme permits time steps about 1.7 times larger than the leapfrog scheme. First results show, that the new scheme is approximately only 10% more expensive.

The results shown include standalone 2-dimensional advection tests, the flow over an idealized mountain to test the dynamics of the LM and a real case study regarding the 24h precipitation on February 20th 2002 in the southwestern part of Germany.

2. Advection Tests

To evaluate the stability, the numerical diffusion properties as well as the splitting error of the new schemes, two different types of 2-dimensional advection tests were carried out.

The first test is described by Durran (1999) and investigates the advection of a tracer in a deformational flow field. Starting with an initial field of the tracer as a cone with a maximum value of 1.0. The results are presented in Figure 1. Figure 1 a shows the isolines of the tracer after one half of the time steps - the point of time with the strongest deformation. In the second half, the flow is reversed and the outcome of the simulation should be as close the to initial field as possible. In this regard the centered difference scheme of 4th-order (Figure 1 d) performs best with virtually no numerical diffusion at all. Unfortunately when actually used in the LM, numerical smoothing through 4th-order artificial horizontal diffusion is necessary. Therefore this has to be taken into account and the result is shown in Figure 1 e. The same is true for the scheme currently used in the operational version of LM - namely the leapfrog scheme combined with 2nd-order centered advection (Figure 1 f). In addition the gain in the maximum allowable time step with the RK-3rd / CD-4th scheme is minor whereas the RK-3rd / UP-5th (Figure 1 b) scheme remains stable using a time step which is about 1.7 times larger. Also the implicit numerical diffusion of the 5th-order scheme sufficiently damps the small scale oscillations. But first real case studies show, that a very small artificial diffusion might be beneficial. The last advection scheme tested is a weighted essentially non oscillating (ENO) scheme (Figure 1 c). In this scheme the fluxes at the cell boundaries are computed in a way to reduce artificial oscillations in the vicinity of steep gradients of the advected field to a minimum. This scheme also permits the greater time step of the UP-5th scheme. But direct comparison with this scheme shows, that the weighted ENO scheme is slightly more diffusive and has a bigger directional splitting error. Last but not least it is computational even more demanding. Nevertheless in the case of steep gradients one gets better results with the ENO scheme which nearly preserves the maximum value.

In Figure 2 the same test is repeated with the TVD variant of the 3rd-order Runge-Kutta scheme. The results shown for 4th-order (Figure 2 a) and 5th-order (Figure 2 b) advection compare well with Figure 1 d and Figure 1 b respectively. Especially the case shown in Figure 1 a is interesting. Here the TVD property of the scheme is apparent and in addition the scheme is more stable than its non-TVD counterpart.

The second test is a standard solid body rotation case. Again the RK-3rd / UP-5th scheme performs quite well (Figure 3) - all in all it seems to be the scheme of choice.

Discretization

(of $\frac{\partial\phi}{\partial t} = -u\frac{\partial\phi}{\partial x}$)

$$\phi_i^{*} = \phi_i^n - \frac{1}{3}\frac{\Delta t}{\Delta x}\,A_i^n \qquad \phi_i^{*} = \phi_i^n - \frac{\Delta t}{\Delta x}\,A_i^n$$

$$\phi_i^{**} = \phi_i^n - \frac{1}{2}\frac{\Delta t}{\Delta x}\,A_i^{*} \qquad \phi_i^{**} = \frac{3}{4}\phi_i^n + \frac{1}{4}\phi_i^{*} - \frac{1}{4}\frac{\Delta t}{\Delta x}\,A_i^{*}$$

$$\phi_i^{n+1} = \phi_i^n - \frac{\Delta t}{\Delta x}\,A_i^{**} \qquad \phi_i^{n+1} = \frac{1}{3}\phi_i^n + \frac{2}{3}\phi_i^{**} - \frac{2}{3}\frac{\Delta t}{\Delta x}\,A_i^{**}$$

Time-Integration:
- 2nd-order Runge-Kutta
- **3rd-order Runge-Kutta** (left)
- **3rd-order TVD-Runge-Kutta** (right)

$$A_i^{4\mathrm{th}} = \frac{u_i}{12}\left[\phi_{i-2} - 8\left(\phi_{i-1} - \phi_{i+1}\right) - \phi_{i+2}\right]$$

$$A_i^{5\mathrm{th}} = \frac{u_i}{60}\left[-\phi_{i-3} + 9\left(\phi_{i-2} - \phi_{i+2}\right) - 45\left(\phi_{i-1} - \phi_{i+1}\right) + \phi_{i+3}\right] + \frac{|u_i|}{60}\left[-\phi_{i-3} + 6\left(\phi_{i-2} + \phi_{i+2}\right) - 15\left(\phi_{i-1} + \phi_{i+1}\right) + 20\phi_i - \phi_{i+3}\right]$$

Advection Schemes:
- 3rd-order upwind
- **4th-order centered differences**
- **5th-order upwind**

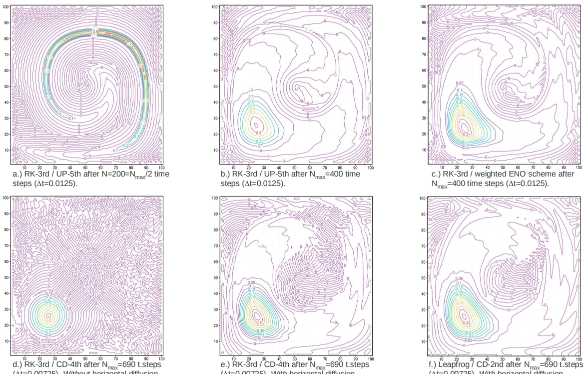

a.) RK-3rd / UP-5th after $N=200=N_{max}/2$ time steps (Δt=0.0125). b.) RK-3rd / UP-5th after N_{max}=400 time steps (Δt=0.0125). c.) RK-3rd / weighted ENO scheme after N_{max}=400 time steps (Δt=0.0125).

d.) RK-3rd / CD-4th after N_{max}=690 t.steps (Δt=0.00725). *Without* horizontal diffusion. e.) RK-3rd / CD-4th after N_{max}=690 t.steps (Δt=0.00725). *With* horizontal diffusion. f.) Leapfrog / CD-2nd after N_{max}=690 t.steps (Δt=0.00725). *With* horizontal diffusion.

Figure 1. Advection of a passive tracer in a nondivergent deformational flow (Durran 1999). Initial tracer field: Cone with a maximum of 1.0.

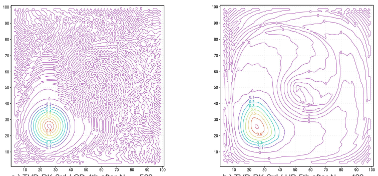

a.) TVD-RK-3rd / CD-4th after N_{max}=500 time steps (Δt=0.01). b.) TVD-RK-3rd / UP-5th after N_{max}=400 time steps (Δt=0.0125).

Figure 2. As in Figure 1.

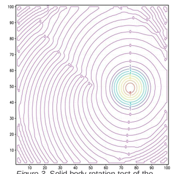

Figure 3. Solid body rotation test of the RK-3rd / UP-5th scheme. Result after 4 revolutions. Initial tracer field: Cone with a maximum of 10.0.

3. Idealized Flow over a Mountain

A further study addresses the simulation of the flow over a bell shaped mountain. The results are shown in Figure 4 - details of the configuration are given in the caption. Comparing the patterns of the mountain wave for the three different schemes shown in Figure 4 a-c, one can see, that the results agree very well especially in respect of the phasing of the wave. There are however slight differences in the amplitude of the wave, with more pronounced downdraft and updraft regions in the lee of the mountain especially in the case of the RK-3rd / UP-5th scheme shown in Figure 4 c. Again this scheme allows a bigger time step of 72 s compared to the operationally used 40 s of the leapfrog scheme. To evaluate the differences in the amplitude a comparison of the results with a linear model is planed. In Figure 4 d again the TVD variant is used. The differences to the non-TVD variant are minor and the statements regarding the amplitude and the stability of the scheme hold here as well.

Figure 4 e shows a cross section in 1000 hPa of the streamwise velocity component for the RK-3rd / UP-5th scheme. The symmetry of the pattern is quite good which should be expected. The same is true for the other schemes.

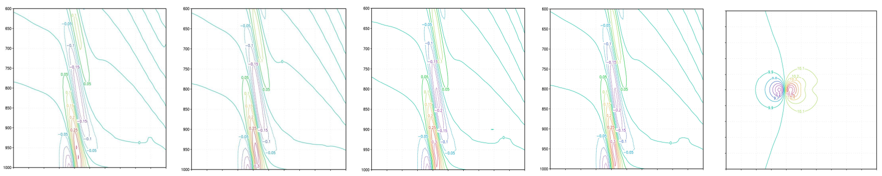

a.) Leapfrog / CD-2nd - vertical cross section of omega. Time step: Δt = 40 s. b.) RK-3rd / CD-4th - vertical cross section of omega. Time step: Δt = 40 s. c.) RK-3rd / UP-5th - vertical cross section of omega. Time step: Δt = 72 s. d.) TVD-RK-3rd / UP-5th - vertical cross section of omega. Time step: Δt = 72 s. e.) RK-3rd / UP-5th - horizontal cross section of u in the 1000 hPa layer. Time step: Δt = 72 s.

Figure 4. Idealized case study of the flow over a bell shaped mountain of 100 m height and a half extension of 28 km. The simulation was initialized using a streamwise velocity of 10 m/s and an isothermal stratification. LM was run with the operational resolution of approximately 7 km without physical parameterizations. Shown are results after a simulation time of 12 h.

4. Case Study of a Precipitation Event in Southwestern Germany

To evaluate the overall performance of the model a 30 h forecast for February 20th, 2002 was done using the various numerical schemes. This case is particularly interesting in regard to the simulated precipitation field. In Figure 5 the observed precipitation in the federal state of Baden-Württemberg from 6 UTC to 30 UTC is given. In this region the observational net is rather dense. Figure 6 shows the simulated 24 h precipitation of the operational version of LM. The apparent problem in the region of the Black Forest with too much precipitation on the windward side rather than on the crest of the mountains and a extremely dry zone in the downdraft area is addressed in a talk of Jan-Peter Schulz at this meeting. In short, the inclusion of the prognostic treatment of rain and snow (Gaßmann 2002), allowing a horizontal drift of this quantities has a very beneficial effect. Especially with increasing resolution, the transport of the hydrometeors is a physical process that has to be taken into account. This is done in the different simulations displayed in Figure 7. Figure 7 a shows the results of the 2-timelevel scheme implemented by Gaßmann (2002). The agreement with the observational data is extremely well. When using the new high-order schemes we get very similar results (Figure 7 b and c) and the question - at least for the precipitation sums presented - which is best, is rather philosophical.

Nevertheless what is remarkable is, that again the RK-3rd / UP-5th scheme and its TVD variant allow a time step of 72 s for the dynamics. Since the moisture variables are treated with a simple Euler-forward scheme, the advection of these quantities is computed twice in one big time step.

To evaluate the efficiency of the RK-3rd / UP-5th scheme it was also run without the prognostic treatment of the precipitation again using a time step of 72 s. Comparison with the Leapfrog scheme (Δt = 40 s) shows, that the new scheme is only about 10% more expensive - further optimization possibilities notwithstanding.

In Figure 8 the same case study is repeated using a finer grid with a resolution of 2.8 km. Only the result for the TVD-RK-3rd / UP-5th scheme is shown. Whereas we get higher maximum values - which is to be expected, the mean precipitation is comparable and even slightly smaller than in the 7 km case. A time step of 36 s is used compared to a value of 20 s for the leapfrog or RK-2nd scheme.

To conclude, this first results look very promising. But naturally further tests have to be performed.

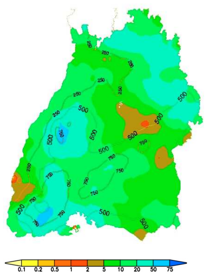

Figure 5. Observed 24 h precipitation in south-western Germany.
02/20/2002 - 06 UTC to 02/21/2002 - 06 UTC
Minimum: 0,5 kg/m² Maximum: 60 kg/m²

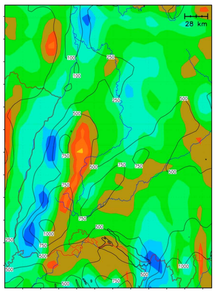

Figure 6. Leapfrog / CD-2nd - Simulated 24 h precipitation for the case given in Figure 5 with the operational version of LM (Resolution: 7 km). No prognostic treatment of snow and rain.

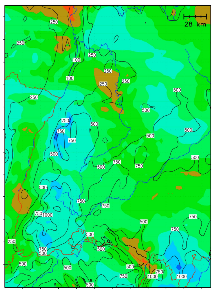

Figure 8. As in Figure 7 but with a resolution of 2.8 km. TVD-RK-3rd / UP-5th - time step: Δt = 36 s.
Min.: 0.95 kg/m² Max.: 95.24 kg/m² Mean: 16,48 kg/m²

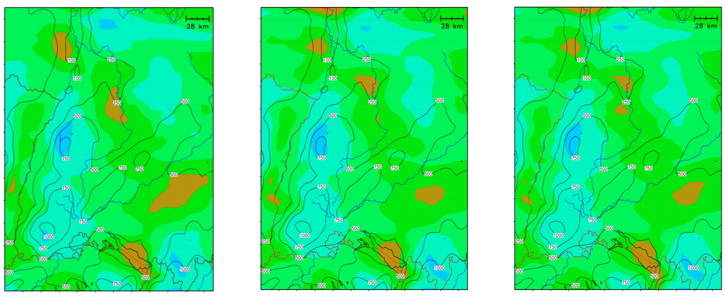

a.) 2-timlevel scheme of Gaßmann (2002) (RK-2nd / UP-3rd) - time step: Δt = 40 s.

b.) RK-3rd / UP-5th - time step: Δt = 72 s.
Min.: 0.73 kg/m² Max.: 72,57 kg/m² Mean: 16,63 kg/m²

c.) TVD-RK-3rd / UP-5th - time step: Δt = 72 s.
Min.: 0.89 kg/m² Max.: 71.33 kg/m² Mean: 16,55 kg/m²

Figure 7. LM simulations of the 24 h precipitation for the case given in Figure 5 using different 2-timelevel schemes (Resolution: 7 km). Prognostic treatment of snow and rain.

References

Durran, D. R. (1999). *Numerical Methods for Wave Equations in Geophysical Fluid Dynamics.* New York: Springer-Verlag, Inc.

Gaßmann, A. (2002). Numerische Verfahren in der nichthydrostatischen Modellierung und ihr Einfluß auf die Güte der Niederschlagsvorhersage. PHD Thesis, Deutscher Wetterdienst, Offenbach am Main.

Shu, C.-W. and S. Osher (1988). Efficient implementation of essentially non-oscillatory shock-capturing schemes. *J. Comput. Phys. 77*, 439-471.

Wicker, L. J. and W. C. Skamarock (2002). Time-splitting methods for elastic models using forward time schemes. *Mon. Wea. Rev. 130*, 2088-2097.